

# Injection of Cerium Oxide Nanoparticles to Treat Spinal Cord Injury in Rats

Zahra Behroozi, PhD, Behnaz Rahimi, MS, Michael R. Hamblin, PhD, Farinaz Nasirinezhad, PhD, Atousa Janzadeh, PhD, and Fatemeh Ramezani, PhD

## Abstract

This study investigated the effects of local injection of cerium oxide nanoparticles (CeONPs) in a rat spinal cord injury (SCI) model. Thirty-six adult male Wistar rats were divided into 4 groups: controls (healthy animals), sham (laminectomy), SCI (laminectomy+SCI induction), and treatment (laminectomy+SCI induction+intrathecal injection of CeONPs immediately after injury). SCI was induced using an aneurysm clip at the T12-T13 vertebral region. Motor performance and pain threshold tests were performed weekly; H&E staining and measurement of cavity sizes were performed 6 weeks after injury. The expression of granulocyte colony-stimulating factor (GCSF), P44/42 MAPK, P-P44/42 MAPK, Tau, myelin-associated glycoprotein(MAG) was evaluated after 6 weeks by Western blot. The Basso, Beattie, and Bresnahan locomotor scoring scales improved in animals receiving CeONPs compared with SCI animals. The cavity sizes were less in the treatment group. GCSF expression was similar in the animals receiving CeONPs compared with the SCI group but the expression of ERK1/ERK2 and phospho-ERK was lower than in the SCI group. Expression levels of Tau and MAG were significantly increased in treated animals compared to the SCI group. These data indicate that the use of CeONPs may improve motor functional recovery in SCI.

**Key Words:** Cerium oxide nanoparticles, Neural cells, Regeneration, Spinal cord injury.

From the Physiology Research Center, Institute of Neuropharmacology, Kerman University of Medical Sciences, Kerman, Iran (ZB); Department of Physiology, School of Medicine, Iran University of Medical Sciences, Tehran, Iran (ZB, BR); Laser Research Centre, Faculty of Health Science, University of Johannesburg, Doornfontein, South Africa (MRH); Physiology Research Center, Faculty of Medicine, Iran University of Medical Sciences, Tehran, Iran (FN); Radiation Biology Research Center, Iran University of Medical Sciences, Tehran, Iran (AJ); and Physiology Research Center, Iran University of Medical Sciences, Tehran, Iran (FR)

Send correspondence to: Fatemeh Ramezani, PhD, Physiology Research Center, Iran University of Medical Sciences, Tehran, Iran; E-mail: ramezani.f@iums.ac.ir; framezani2014@gmail.com

Zahra Behroozi and Behnaz Rahimi are co-first authors.

Atousa Janzadeh and Fatemeh Ramezani contributed equally to the work.

The work was funded by the Iran University of Medical Sciences award number 98-4-99-16788 to FR and NIH #RO1AI050875 and R21AI121700 to MRH.

## INTRODUCTION

Spinal cord injury (SCI) is one of the most common and complex clinical problems worldwide and leads to many debilitating manifestations including motor dysfunction, sensory disorders, and neuropathic pain (1). In SCI, the initial stage begins immediately after injury, which causes the death of some nerve cells due to direct compression or reduced blood flow (2). However, major injuries continue to occur in the secondary injury phase. These include apoptosis, inflammation, microglial activation, demyelination, and axonal degeneration (3, 4). Axonal regeneration is a key step in the SCI recovery process. However, the inability of axons in the adult central nervous system (CNS) to regenerate has so far prevented adequate restorative treatment for SCI. Several efforts have been made to promote regeneration of the spinal cord after injury and some progress has been made (5, 6).

Nevertheless, the therapeutic effects and overall outcomes in SCI patients have been disappointing to date. This requires the implementation of new and effective methods for treating SCI that may allow restoration of functionally active neuronal cells, repair, and subsequent reduction of neuropathic pain (7, 8).

Reactive oxygen species (ROS) increase dramatically during the inflammatory process following SCI, and are thought to be a major cause of secondary injury, nerve cell damage, axonal degeneration, neuropathic pain, and motor dysfunction (7). Therefore, reducing ROS levels are expected to improve the biological function of damaged nerve cells. Previous studies have shown that ROS-reducing approaches can reduce nerve cell apoptosis, and also improve motor function.

Cerium oxide is a rare earth metal that can exist in both 3<sup>+</sup> and 4<sup>+</sup> oxidation states. Cerium oxide exists as both CeO<sub>2</sub> and Ce<sub>2</sub>O<sub>3</sub> in bulk state; however, at the nanoscale level, cerium oxide is a mixture of cerium III and cerium IV on the surface of nanoparticles that have the ability to undergo redox reactions (8, 9). As the diameters of nanoparticle decrease, the number of Ce (III) sites on the surface increases and some oxygen atoms are lost (oxygen vacancies). This results in increases in catalytic activity. Cerium oxide nanoparticles (CeONPs) are a nontoxic nanomaterial that can act as a catalyst for redox reactions and ROS destruction (10, 11). In addition,

tion, CeONPs are thought to mimic the properties of some enzymes such as, superoxide dismutase, catalase, peroxidase, oxidase, as well having the ability to quench hydroxyl and nitric oxide radicals (12, 13). Because of the antioxidant properties of CeONPs, they are expected to help nerve regeneration after SCI. The effect of CeONPs has been investigated for the recovery of nerve tissue in vitro (14), in sciatic nerve crush injury in vivo (15), and in functional recovery after SCI (16). Despite the fact that CeONPs can act as potent antioxidants and are beneficial for SCI, there are no reports on the capacity of CeONPs to help neuron regeneration after SCI. In this study we investigated the effects of 10  $\mu$ L of CeONPs (1000  $\mu$ g/ml) injected into the lesion area, on factors relating to repair and nerve regeneration after SCI in rats.

## MATERIALS AND METHODS

### Study Design

Adult male Wistar SD rats (weighing 150–185 g,  $n=36$ ) were kept under controlled conditions (12 hours of light and 12 hours of darkness, 6 AM to 6 PM) and temperature ( $22 \pm 2^\circ\text{C}$ ) in the animal laboratory of Iran University of Medical Sciences. Four rats were placed in each cage and the animals in all groups had free access to water and pelleted chow. The experimental animal research protocol was approved by the ethics committee of Iran University of Medical Sciences (98-4-99-16788). In this study, the animals were randomly divided into 4 groups ( $n=9$ ): (i) control group (healthy animals); (ii) sham group (laminectomy); (iii) 3-SCI group (laminectomy + SCI induction); and (iv) treatment group (laminectomy + SCI + intraspinal injection of CeONPs immediately after injury).

### SCI Model Induction

The method of SCI induction and nanoparticles injection as previous study (17). Briefly, the animals were anesthetized by injection of a mixture of ketamine and xylazine (100 mg/kg and 10 mg/kg i.p., respectively). After identifying areas T12 to T13, the skin at the site of surgery was shaved, cleaned, and disinfected. A midline incision was performed, the skin and superficial muscles were separated, and the spinal cord was exposed by a laminectomy. The last rib was an important guide for confirming the location of the injury in the T13 vertebra (18). We then applied an aneurysm clip (force = 20 g/cm<sup>2</sup>, FST company) onto the spinal cord for 90 seconds. Muscles and skin were closed by separate sutures (0.3 suture thread). Postoperatively, tetracycline was sprayed at the injury site and 70% alcohol in a cage daily for 1 week to prevent infection. The bladders of animals in the third and fourth groups were emptied manually twice a day until the return of spontaneous reflex (between 3 and 7 days after SCI).

### CeONPs Injection

After induction of SCI, 10  $\mu$ L of sonicated CeONPs (1000  $\mu$ g/ml) (16) (purchased from Sigma Aldrich No. 796077) were immediately inoculated into the dorsal horn of the spinal cord. The Hamilton syringe was then immobile in a

stereotaxic device and a glass micropipette attached to a stereotaxic injector. CeONPs were injected into 4 spots (2 spots on the right and 2 spots on the left side of the lesion, the depth of injection was 1 mm from the dura surface). About 2.5  $\mu$ L of nanoparticles were injected at each site. Then, the muscles and skin were sewed and the animals were returned to their cages.

### Behavioral Study

Behavioral tests were performed every week for 6 weeks after SCI induction. The Basso, Beattie, and Bresnahan (BBB) locomotor scoring scale was used to rate hind limb motor function (19). The rats were placed in a container 120 cm in diameter and were studied and rated for 4 minutes. The evaluation included joint motions, coordination, paw placement, and toe clearance. A score of 0 indicated a complete paralysis; a score of 21 indicated walking as normal animals (19). After 6 weeks, the rats were deeply anesthetized and the spinal tissue in the T12 to T13 region was prepared by perfusion for hematoxylin and eosin (H&E) staining. Additionally, animals were killed to obtain a fresh injured tissue (T12-T13) harvested for Western blotting.

### Transcardiac Perfusion and Spinal Fixation for Tissue Assessment

In the sixth week, after the last behavioral assessment, the animals underwent transcardiac perfusion to stabilize the spinal cord for tissue removal. For this purpose, the animal was first deeply anesthetized by intraperitoneal injection of a mixture of ketamine and xylazine and then fixed on a surgical board. The needle of the perfusion system was inserted into the left ventricle from the apex of the heart and the fixative solution (4% paraformaldehyde in 0.1 M phosphate buffer pH 7.2–7.4) was circulated in the arteries for 35–40 minutes. After these steps, the spinal cord was removed from the vertebral column and placed in 4% paraformaldehyde to ensure tissue stabilization, until dissection. The spinal cord was dissected in the T12-T13 vertebral region and postfixed in 4% paraformaldehyde for 24 hours. The tissue samples were embedded in paraffin and 5- $\mu$ m-thick sections were cut for tissue staining.

### Hematoxylin and Eosin Staining

Histological H&E staining was used to confirm the SCI model and measure the size of the SCI-induced cavity. H&E staining was done for calculation of cavity size (20). Five sections (from injury site with 100- $\mu$ m intervals) from each rat were collected and the percentages of cavity size and percentage of myelin assessment were calculated separately by Image J software using the following formula:

$$\text{Percent of cavity size} = \frac{\text{Cavity size (pixel)}}{\text{Total area of the section (pixel)}} \times 100.$$

### Western Blotting

About 0.5 cm of spinal cord tissue ( $n=3$  in each group) was rapidly excised, and stored for protein extraction and

Western blotting at  $-80^{\circ}\text{C}$ . For every 100 mg of tissue, 300  $\mu\text{L}$  of RIPA buffer were added and the mixture was left on ice for 30 minutes and then homogenized. Tissues were centrifuged (13 000g, 30 minutes,  $4^{\circ}\text{C}$ ). The supernatants were isolated and the protein concentration was estimated using a Nanodrop spectrophotometer (Thermo Fisher Scientific, Waltham, MA). In the next step, supernatants were used for Western blotting. The lysates (containing 50  $\mu\text{g}$  of protein) were placed on SDS gel and the proteins were separated at 15 V and transferred to a polyvinylidene-fluoride (PVDF) membrane for 25 minutes. After blocking with a fresh blocking buffer (5% skim milk and 0.1% Tween-20 in Tris-buffered saline, pH 7.4) at room temperature for 2 hours, the membranes were incubated with the primary antibodies including granulocyte colony-stimulating factor (GCSF) antibody (orb308858, MW: 90 kDa), P44/42 MAPK (ERK1/ERK2) antibody (1:1000, 9102S, MW: 42–44 kDa), phospho-P44/42 MAPK (ERK1/ERK2) (4376S), total Tau antibody (1/1000, orb158145, MW: 52/79 kDa), total myelin-associated glycoprotein (MAG) (1/1000, orb536682, MW: 63 kDa),  $\beta$ -actin antibody (1:500, sc-47778, MW: 45 kDa) overnight. The membranes were then washed with TBST (for 10, 3, and 3 minutes), and incubated with goat horseradish peroxidase conjugated IgG (1/1000, sc-516102). Protein bands were detected by enhanced luminescence chemistry and captured by the ChemiDoc imaging system.  $\beta$ -Actin was the internal standard for the Western blotting. The results were quantified by Image J software.

## Statistical Analysis

Statistical analysis of the results and all behavioral, molecular, and histological assessments were performed blindly and the researchers were not aware of the animal groupings. Statistical software SPSS 22.0 and Graph Pad Prism 8.0 were used for analysis. Behavioral data were analyzed using repeated measure ANOVA with Bonferroni post hoc test. Moreover, one-way ANOVA was used to evaluate the proteins. Any trial done 3 times and data were presented as mean  $\pm$  SD. In all analyses,  $p < 0.05$  was considered significant.

## RESULTS

Six weeks after intraspinal CeONP injection, 1 rat died due to surgical complications and was replaced in the study. Data from 36 animals were included in the final analysis.

### Effectiveness of CeONP on Locomotor Function Recovery

The results showed that SCI induction led to a reduction in BBB score in the 6-week experiment, compared to baseline measurement (DF = 18 199;  $F = 77.46$ ;  $p < 0.0001$ ). No significant difference was observed between the sham and control group from the first week after SCI to the sixth week. A significant reduction in motor function in SCI animals began in the first week and continued until the end of the study compared to the control group ( $p < 0.0001$ ). The BBB score in animals, which received CeONPs improved at 1 week after

injury in comparison with SCI animals ( $p < 0.0001$ ) and this improvement continued up to the sixth week. However, the locomotor performance of CeONPs treatment group did not reach the control level by the sixth week ( $p = 0.0001$ ) (Fig. 1A).

### Cavity Formation after SCI

Cavitation was visualized after SCI by H&E staining (Fig. 2). The total cavity area (%) was markedly reduced in the group that received CeONPs injection. Only very small cavities were identified within the lesions in the treatment group. Figure 2 shows the difference in the percentage area of cavities at 28 days after SCI in the groups, control, sham, CeONPs, and SCI. The % cavity size was significantly different between CeONPs treatment and SCI groups ( $p < 0.001$ ).

### Effects of CeONPs on the GCSF

The results showed that there was a significant difference in the expression of GCSF between the groups in the sixth week of the experiment (DF = 3;  $F = 7.227$ ;  $p = 0.011$ ). The GCSF expression was significantly lower in the SCI group ( $0.0577 \pm 0.016$ ) compared to the control group ( $0.7177 \pm 0.028$ ,  $p = 0.038$ ). The expression level of GCSF was increased in rats receiving CeONPs, but its increase was not statistically significant ( $0.19 \pm 0.015$ ) compared to the SCI group (Fig. 3).

### Effects of CeONPs on the Expression of P44/42MAPK (ERK1/ERK2)

The results showed a significant difference in the expression of P44/42 MAPK (ERK1/ERK2) between the groups in the sixth week (DF = 3;  $F = 23.149$ ;  $p < 0.0001$ ). The P44/42 MAPK expression was significantly higher in the SCI group ( $0.515 \pm 0.432$ ) compared to the control ( $0.1543 \pm 0.066$ ,  $p = 0.002$ ) and sham ( $0.078 \pm 0.35$ ,  $p < 0.0001$ ) groups. The expression level of P44/42 MAPK in animals receiving CeONPs was significantly lower ( $0.086 \pm 0.002$ ) compared to the SCI group ( $p < 0.0001$ ). In addition, there was no significant difference in P44/42 MAPK expression between the treatment and control group (Fig. 3B).

### Effects of CeONPs on the Expression of Phospho-P44/42MAPK (ERK1/ERK2)

The result showed significant difference in phospho-ERK1/ERK2 expression between groups in the sixth week of the experiment (DF = 3;  $F = 5.211$ ;  $p = 0.028$ ). The phospho-ERK1/ERK2 expression was significantly increased in the SCI group ( $1.492 \pm 0.367$ ) compared to the control group ( $0.5513 \pm 0.566$ ,  $p = 0.046$ ). The expression level of phospho-ERK1/ERK2 protein in animals which received CeONPs was significantly lower ( $0.545 \pm 0.51$ ) compared to the SCI group ( $p = 0.045$ ). In addition, there was no significant difference in phospho-ERK1/ERK2 expression between the treatment and control group (Fig. 3C).

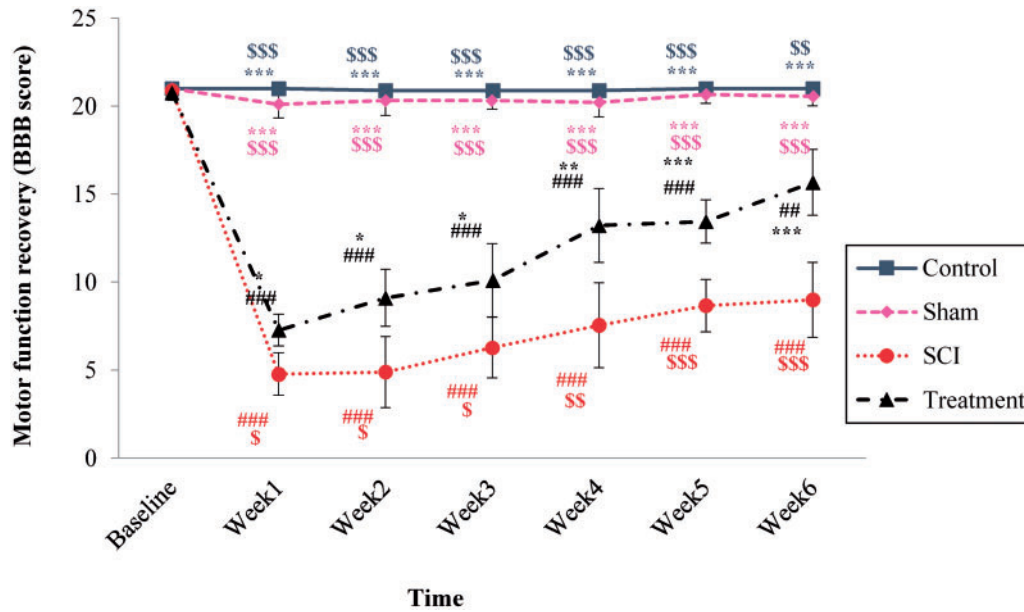


**FIGURE 1.** The effect of CeONP injection immediately after the induction of spinal cord injury (SCI) on locomotor function recovery (BBB score). Data are mean±SD (n=9 in each group). \*p<0.05, \*\*p<0.01, \*\*\*p<0.001 versus SCI groups. #p<0.05, ##p<0.01, ###p<0.001 versus control group. §p<0.05, §§p<0.01, §§§p<0.001, versus group that received CeONPs.

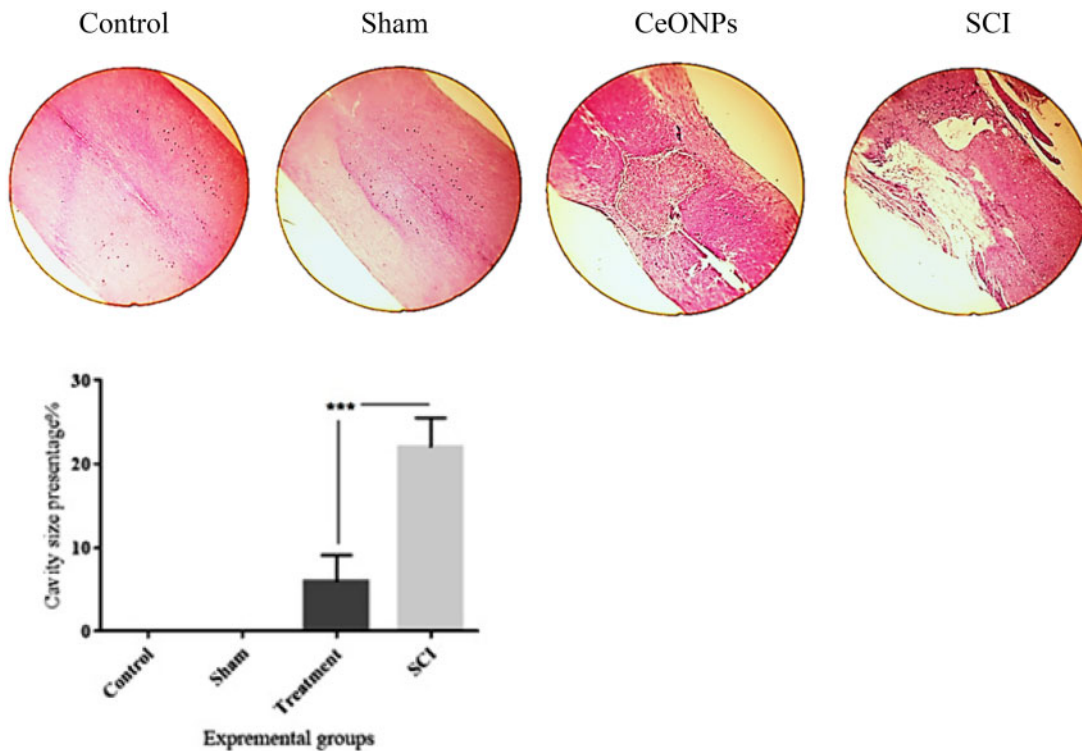


**FIGURE 2.** Histological staining (H&E) of longitudinal sections of the spinal cord (5µm) showing the % cavity size in control, sham, SCI, and treatment group. As shown in the graph, at the sixth week after SCI induction, the cavity size in the SCI group was significantly larger than that in the CeONP group. Data are expressed as mean±SD (\*\*p < 0.001).

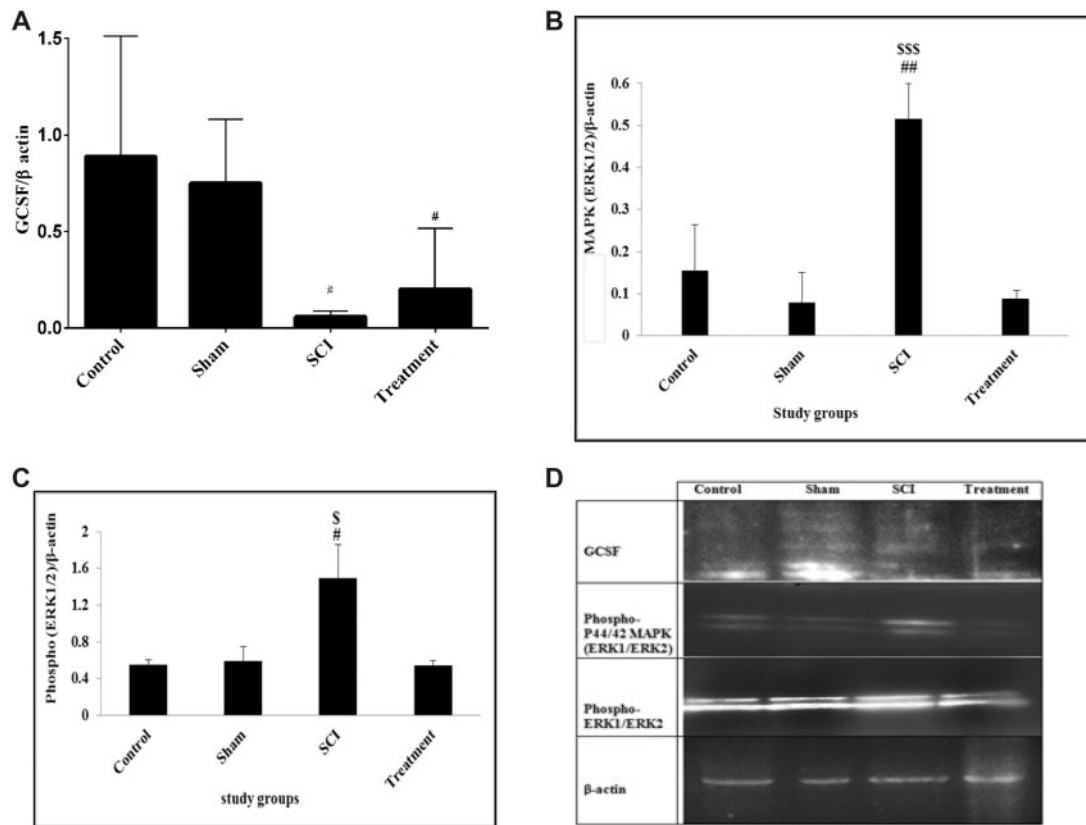


**FIGURE 3.** Expression of granulocyte colony-stimulating factor (GCSF), P44/42 MAPK (ERK1/ERK2) and phospho-P44/42 MAPK (ERK1/ERK2) proteins by Western blot. The test was performed thrice on proteins and integrated optical density of each band was normalized to corresponding β-actin level. GCSF protein (**A**); phospho-P44/42 MAPK (ERK1/ERK2) protein (**B**); phospho-ERK1/ERK2 protein (**C**); Western bolt bands of proteins (**D**). Graphical data are shown as the mean ± SD. ##p < 0.01, #p < 0.05 compared to control group and \$\$\$p < 0.001, \$p < 0.05 compared to treatment group.

### Effects of CeONPs on the Expression of Tau Protein

The result showed a significant difference in the expression of Tau between groups at the sixth week of the experiment (DF = 3; F = 8.651; p = 0.007). Tau expression was significantly lower in the SCI group (0.286 ± 0.04) compared to the control group (0.717 ± 0.022, p = 0.017). The expression level of Tau protein in rats which received CeONPs (0.7 ± 0.96) was significantly higher compared to SCI rats (p = 0.02). There was no significant difference in Tau expression between treatment and control groups (Fig. 4A).

### Effects of CeONPs on the Expression of MAG

The result showed a significant difference in the expression of MAG between groups at the end study (df = 3, F = 6.245; p = 0.017). MAG expression was significantly lower in the SCI group (0.127 ± 0.097) compared to the control group (1.29 ± 0.385, p = 0.026). The expression level of MAG protein in rats, which received CeONPs (1.2 ± 0.054) was significantly higher compared to the SCI group (p = 0.037). There was no significant difference in Tau expression between treatment and control group (Fig. 4B).

### DISCUSSION

In this study, SCI induction caused motor impairment and cavity formation. Treatment with CeONPs improved parameters of neuron regeneration, the locomotor ability, and reduced size of the cavity. These findings indicate the effectiveness of CeONPs as an antioxidant, which may improve some of the important clinical manifestations of SCI such as locomotor impairment. After SCI, a lack of growth factors and the suppression of axonal outgrowth due to the secretion of inhibitory molecules, contribute to the devastating consequences of SCI such as permanent disability.

ERK1/ERK2 are increased after SCI. Studies have shown that the activation of ERK signaling pathway is associated with spinal cord degeneration and dysfunction induced by SCI in rats. ERK2 activation may contribute to pathological and functional deficits following SCI (21). When SCI is in the acute phase, increased nitric oxide production not only increases the level of ERK1/2 phosphorylation, but also increases the level of activated protein kinases in microglia/macrophages within the affected area. In addition, these proteins play an important role in neuronal degeneration following acute SCI (22). Therefore, motor dysfunction will occur and a cavity is created in the lesion area. However, after treat-

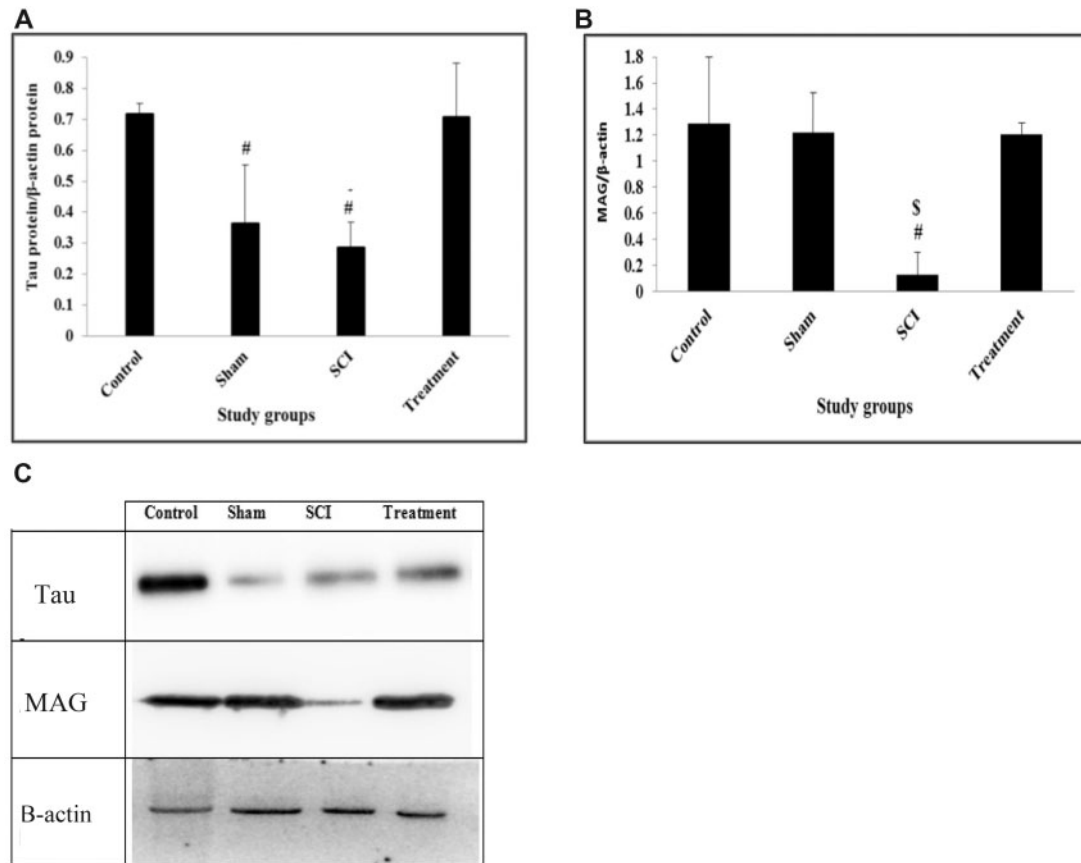


**FIGURE 4.** Western-blot analysis of expression of Tau and MAG proteins. The test was performed 3 times and integrated optical density of each band was normalized to the corresponding  $\beta$ -actin level. Total tau (**A**); Total MAG (**B**); Western blotting images (**C**). Graphical data are shown as the mean  $\pm$  SD. <sup>#</sup> $p < 0.05$  compared to control group and <sup>\$</sup> $p < 0.05$  compared to CeONPs group.

ment with CeONPs, their expression returned to the normal level. ERK1/2 inhibitors can significantly reduce secondary SCI and improve neurological function in rats (23, 24).

Previous studies have reported that antioxidants were not able to control inflammation or reduce ROS generation by decreasing ERK1/ERK2 (25, 26), whereas we found that CeONPs prevented an increase in ERK1/ERK2. The CeONPs may allow them to remain in place for a long time in the injured region of the spinal cord, to reduce the formation of cavities.

MAG is a protein present on the surface of oligodendrocytes. It participates in the formation of glial scar and promotes cavity formation. MAG is thought to inhibit axon growth via binding to Nogo receptors (chondroitin sulfate proteoglycan receptors) (27, 28). It is suggested that MAG plays a dual role, that is either promoting or inhibiting neuronal outgrowth depending on the age of the neuron. MAG inhibits most mature neurons, but plays a regenerative role in the growth of new axons in damaged white matter (27, 29). Studies have demonstrated the inhibitory role of MAG, and suggested that MAG could be partly responsible for the lack of CNS neuron regeneration in vivo (30). Other studies have shown that MAG knockout mice failed to show axon regener-

ation in the optic nerve, or the CST, suggesting that MAG may be required for sprouting of corticospinal axons (31). On the other hand, MAG is a transmembrane glycoprotein expressed in the axonal membrane of oligodendrocytes between axons and the inner myelin sheath, and has a function in the maintenance of myelinated axons in the adult nervous system (5, 29). Therefore, a reduction in MAG could indicate damage and detachment of myelinated axons in the SCI model (29, 32).

In the present study, induction of SCI reduced MAG expression. Therefore, it is possible that the lower MAG expression led to cavity growth and glial scar formation in the chronic phase of SCI. The injection of antioxidant CeONPs led to increased MAG expression, which may stimulate the growth of the axons after injury (33). On the other hand, the increased MAG expression may have been caused by inhibiting progressive cell damage and preserving the environment in the spinal cord.

Tau is a major microtubule associated protein that contributes to a number of cellular processes, including axonal trafficking, myelination, synaptic plasticity, and is also involved in pain perception (34, 35). Tau is a cytoplasmic neuronal marker that maintains the stability of axons, and its presence in CSF or serum is considered to be an indicator of

axonal degeneration or damage in conditions such as Alzheimer disease or SCI (36–38). According to reports, in the first hours and days after SCI, Tau expression remains high, indicating that the process of neuronal death and axonal injury continues (38, 39). In the chronic phase of SCI, we observed a decrease in Tau expression compared to the control group.

In healthy neural tissue, Tau facilitates microtubule stabilization within cells and is particularly abundant in neurons (40). In agreement with this, we observed high levels of Tau protein in the control group. Administration of CeONPs may have prevented the reduction of Tau protein in neurons due to the inhibition of neuronal damage.

There are many different studies that have confirmed the antioxidant properties of CeONPs in different tissues and in serum (41–43). In a study by Kim et al in 2017, they showed under conditions similar to our experiment, that injection of the same amount of CeONPs could reduce the ROS levels at the lesion site after SCI. Oxidative stress and ROS production is often associated with sustained activation of the ERK1/2 pathway. ROS-induced ERK1/2 activation (increase of P-ERK1/2) has been shown in a wide variety of cells including neurons, and may promote neuronal death (44). ROS is a cellular stress that can modulate Tau phosphorylation, and several antioxidants have been tested in different models of tauopathy, with some interesting therapeutic effects. On the other hand, the accumulation of hyperphosphorylated Tau has been shown to cause oxidative stress (45). Therefore, the effect of CeONPs, on the neural markers ERK1/2 and Tau, could possibly be explained by its ROS scavenging properties. The expression of GCSF, which is neuroprotective and a stimulator for nerve regeneration (46), was higher in the treatment group compared to the SCI group, but this increase was not statistically significant in our study.

In conclusion, we found that CeONPs injected into the injured spinal cord helped to the regeneration of neurons, improved the functional recovery and decreased the injury cavity size. The mechanisms are proposed to be the inhibition of oxidative stress, leading to the restoration of neurodegenerative factors such as MAG, Tau, and ERK1/2 back to normal levels. Further studies are warranted before clinical trials can be designed.

## REFERENCES

- James SL, Theadom A, Ellenbogen RG, et al. Global, regional, and national burden of traumatic brain injury and spinal cord injury, 1990–2016: A systematic analysis for the Global Burden of Disease Study 2016. *Lancet Neurol* 2019;18:56–87
- Oyinbo CA. Secondary injury mechanisms in traumatic spinal cord injury: A nugget of this multiply cascade. *Acta Neurobiol Exp (Wars)* 2011;71:281–99
- Kanno H, Ozawa H, Sekiguchi A, et al. The role of mTOR signaling pathway in spinal cord injury. *Cell Cycle* 2012;11:3175–9
- Ahuja CS, Wilson JR, Nori S, et al. Traumatic spinal cord injury. *Nat Rev Dis Primers* 2017;3:1–21
- Ueno M, Yamashita T. Strategies for regenerating injured axons after spinal cord injury –Insights from brain development. *Biologics* 2008;2:253–64
- Tran AP, Warren PM, Silver J. The biology of regeneration failure and success after spinal cord injury. *Physiol Rev* 2018;98:881–917
- Luo W, Wang Y, Lin F, et al. Selenium-doped carbon quantum dots efficiently ameliorate secondary spinal cord injury via scavenging reactive oxygen species. *Int J Nanomedicine* 2020;15:10113–25
- Singh KRB, Nayak V, Sarkar T, et al. Cerium oxide nanoparticles: Properties, biosynthesis and biomedical application. *RSC Adv* 2020;10:27194–214
- Dhall A, Self W. Cerium oxide nanoparticles: A brief review of their synthesis methods and biomedical applications. *Antioxidants* 2018;7:1–13
- Celardo I, Traversa E, Ghibelli L. Cerium oxide nanoparticles: A promise for applications in therapy. *J Exp Ther Oncol* 2011;9:47–51
- Datta A, Mishra S, Manna K, et al. Pro-oxidant therapeutic activities of cerium oxide nanoparticles in colorectal carcinoma cells. *ACS Omega* 2020;5:9714–23
- Xu C, Qu X. Cerium oxide nanoparticle: A remarkably versatile rare earth nanomaterial for biological applications. *NPG Asia Mater* 2014;6:e90
- Singh S. Cerium oxide based nanozymes: Redox phenomenon at biointerfaces. *Biointerphases* 2016;11:04B202
- Dong L, Kang X, Ma Q, et al. Novel approach for efficient recovery for spinal cord injury repair via biofabricated nano-cerium oxide loaded PCL with resveratrol to improve in vitro biocompatibility and autorecovery abilities. *Dose-Response* 2020;18:1–18
- Soluki M, Mahmoudi F, Abdolmaleki A, et al. Cerium oxide nanoparticles as a new neuroprotective agent to promote functional recovery in a rat model of sciatic nerve crush injury. *Br J Neurosurg* 2020;1–6
- Kim JW, Mahapatra C, Hong JY, et al. Functional recovery of contused spinal cord in rat with the injection of optimal-dosed cerium oxide nanoparticles. *Adv Sci Lett* 2017;4:1–13
- Behroozi Z, Ramezani F, Janzadeh A, et al. Platelet-rich plasma in umbilical cord blood reduces neuropathic pain in spinal cord injury by altering the expression of ATP receptors. *Physiol Behav* 2021;228:113186
- Moonen G, Satkunendrarajah K, Wilcox JT, et al. A new acute impact-compression lumbar spinal cord injury model in the rodent. *J Neurotrauma* 2016;33:278–89
- Basso DM, Beattie MS, Bresnahan JC. A sensitive and reliable locomotor rating scale for open field testing in rats. *J Neurotrauma* 1995;12:1–21
- Feldman AT, Wolfe D. Tissue processing and hematoxylin and eosin staining. *Histopathology* 2014;1180:31–43
- Yu C-G, Yeziarski RP, Joshi A, et al. Involvement of ERK2 in traumatic spinal cord injury. *J Neurochem* 2010;113:131–42
- Zhu S, Yang B, Li S, et al. Protein post-translational modifications after spinal cord injury. *Neural Regen Res* 2021;16:1935–43
- Genovese T, Esposito E, Mazzon E, et al. Evidence for the role of mitogen-activated protein kinase signaling pathways in the development of spinal cord injury. *J Pharmacol Exp Ther* 2008;325:100–14
- Xu J, Cheng S, Jiao Z, et al. Fire needle acupuncture regulates Wnt/ERK multiple pathways to promote neural stem cells to differentiate into neurons in rats with spinal cord injury. *CNS Neurol Disord Drug Targets* 2019;18:245–55
- Kyaw M, Yoshizumi M, Tsuchiya K, et al. Antioxidants inhibit JNK and p38 MAPK activation but not ERK 1/2 activation by angiotensin II in rat aortic smooth muscle cells. *Hypertens Res* 2001;24:251–61
- Kyaw M, Yoshizumi M, Tsuchiya K, et al. Atheroprotective effects of antioxidants through inhibition of mitogen-activated protein kinases. *Acta Pharmacol Sin* 2004;25:977–85
- Tang BL. Inhibitors of neuronal regeneration: Mediators and signaling mechanisms. *Neurochem Int* 2003;42:189–203
- Janzadeh A, Sarveazad A, Yousefifard M, et al. Combine effect of Chondroitinase ABC and low level laser (660 nm) on spinal cord injury model in adult male rats. *Neuropeptides* 2017;65:90–9
- Lee JK, Zheng B. Role of myelin-associated inhibitors in axonal repair after spinal cord injury. *Exp Neurol* 2012;235:1–7
- Mukherjee N, Ghosh S. Myelin associated inhibitory proteins as a therapeutic target for healing of CNS injury. *ACS Chem Neurosci* 2020;11:1699–700
- Bartsch U, Bandtlow CE, Schnell L, et al. Lack of evidence that myelin-associated glycoprotein is a major inhibitor of axonal regeneration in the CNS. *Neuron* 1995;15:1375–81
- Lopez PHH. Role of myelin-associated glycoprotein (Siglec-4a) in the nervous system. *Adv Neurobiol* 2014;245–62
- Schubert D, Dargusch R, Raitano J, et al. Cerium and yttrium oxide nanoparticles are neuroprotective. *Biochem Biophys Res Commun* 2006;342:86–91
- Sotiropoulos I, Lopes AT, Pinto V, et al. Selective impact of tau loss on nociceptive primary afferents and pain sensation. *Exp Neurol* 2014;261:486–93

35. Techne B. Neural Cell Markers [Internet]. Available at: <https://resources.rndsystems.com/images/site/rnd-systems-neural-markers-br2.pdf>
36. Szalardy L, Zadori D, Simu M, et al. Evaluating biomarkers of neuronal degeneration and neuroinflammation in CSF of patients with multiple sclerosis—Osteopontin as a potential marker of clinical severity. *J Neurol Sci* 2013;331:38–42
37. Fossati S, Ramos J, Debure L, et al. Plasma tau complements CSF tau and P-tau in the diagnosis of Alzheimer's disease. *Alzheimer's Dement* 2019;11:483–92
38. Nakhjiri E, Vafaee MS, Hojjati SMM, et al. Tau pathology triggered by spinal cord injury can play a critical role in the neurotrauma development. *Mol Neurobiol* 2020;57:4845–55
39. KwonBK, StammersAMT, BelangerLM, et al. Cerebrospinal fluid inflammatory cytokines and biomarkers of injury severity. *J Neurotrauma* 2010;27:669–82
40. Sato C, Barthélemy NR, Mawuenyega KG, et al. Tau kinetics in neurons and the human central nervous system. *Neuron* 2018;97:1284–98.e7
41. SepanjniaA, GhasemiH, MohseniR, et al. Effect of cerium oxide nanoparticles on oxidative stress biomarkers in rats' kidney, lung, and serum. *Iran Biomed J* 2020;24:251–6
42. Khorrami MB, Sadeghnia HR, Pasdar A, et al. Antioxidant and toxicity studies of biosynthesized cerium oxide nanoparticles in rats. *Int J Nanomedicine* 2019;4:2915–26
43. Hirst SM, Karakoti A, Singh S, et al. Bio-distribution and in vivo antioxidant effects of cerium oxide nanoparticles in mice. *Environ Toxicol* 2013;28:1–12
44. Subramaniam S, Unsicker K. ERK and cell death: ERK1/2 in neuronal death. *FEBS J* 2010;277:22–9
45. Alavi Naini SM, Soussi-Yanicostas N. Tau hyperphosphorylation and oxidative stress, a critical vicious circle in neurodegenerative tauopathies. *Oxid Med Cell Longev* 2015;2015:151979
46. Chen HPÆC, Ho Æ, Hwang MLÆS, et al. Combination of G-CSF administration and human amniotic fluid mesenchymal stem cell transplantation promotes peripheral nerve regeneration. *Neurochem Res* 2009;34:518–27